



1 A Pan-Arctic Pigment Database for Phytoplankton and 2 Sea-Ice Algae

3

4 Authors

5 Asta C. Heidemann¹, Alexander Hayward², Philipp Assmy³, Atreya Basu⁴, Astrid
6 Bracher^{5,6}, Giulia Castellani⁶, Giacomo Ditullio⁷, Katarzyna Dragańska-Deja⁸, Amane
7 Fujiwara⁹, Glaucia Moreira Fragoso¹⁰, Jacob Høyer², Jiwoon Hwang¹¹, Morten Iversen⁵,
8 Anabel von Jackowski¹², Thomas Juul-Pedersen¹³, Piotr Kowalczyk⁸, Youngju Lee¹⁴,
9 Atsushi Matsuoka¹⁵, Alenya Merz^{13,16}, C. J. Mundy¹⁷, Else Ostermann¹³, Ilka Peeken⁵, Matt
10 Pinkerton¹⁸, Joanna Stoń-Egiert⁸, Antonia U. Thielecke⁵, Gaëlle Veyssiere¹⁹, Hongyan Xi⁵,
11 Eun Jin Yang¹⁴ & Rafael Gonçalves-Araujo¹

12

13 Institution

14 ¹National Institute of Aquatic Resources, Technical University of Denmark (DTU Aqua),
15 Kgs. Lyngby, Denmark

16 ²Danish Meteorological Institute

17 ³Norwegian Polar Institute, Fram Centre, Tromsø, Norway

18 ⁴Centre for Earth Observation Science, University of Manitoba, Winnipeg, Canada

19 ⁵Alfred-Wegener-Institute Helmholtz Center for Polar and Marine Research (AWI),
20 Bremerhaven, Germany

21 ⁶Institute of Environmental Physics (IUP), University Bremen (UB), Bremen, Germany

22 ⁷University of Charleston, Grice Marine Laboratory

23 ⁸Institute of Oceanology Polish Academy of Sciences, Sopot, Poland

24 ⁹Institute of Arctic Climate and Environment Research, Japan Agency for Marine-Earth
25 Science and Technology, Yokosuka, Japan

26 ¹⁰SINTEF Ocean, Department of Climate and Environment, Trondheim, Norway, 7041

27 ¹¹University of California, Berkeley, USA

28 ¹²Stockholm University, Stockholm, Sweden

29 ¹³Greenland Climate Research Centre (GCRC), Greenland Institute of Natural
30 Resources (GINR), Nuuk, Greenland



- 31 ¹⁴Korea Polar Research Institute, Incheon, Republic of Korea
32 ¹⁵Institute for the Study of Earth, Oceans, and Space, University of New Hampshire, USA
33 ¹⁶Groningen Institute for Evolutionary Life Sciences, University of Groningen, Groningen,
34 Netherlands
35 ¹⁷Centre for Earth Observation Science, Faculty of Environment, Earth and Resources,
36 University of Manitoba, Winnipeg, Manitoba, Canada
37 ¹⁸Earth Sciences New Zealand, Wellington, New Zealand
38 ¹⁹British Antarctic Survey, Cambridge, Cambridgeshire, UK

39

40 Correspondence to: Asta C. Heidemann (aheidem@aqu.dtu.dk), Alexander Hayward
41 (algh@dmi.dk) and Rafael Gonçalves-Araujo (rafgo@aqu.dtu.dk)

42

43 Abstract

44 Climate change has dramatically altered the Arctic seas with significant decrease in sea
45 ice extent and thickness and warming water temperature. The ecological impacts of
46 such change have been described for many parts of the Arctic Ocean, but long-term
47 records of biological indicators are still missing. Among those, photosynthetic and
48 accessory pigments are one of the key tools that aid quantification of phytoplankton
49 and sea-ice algae biomass and characterisation of community composition. To address
50 this gap, we present the first pan-Arctic compilation of in situ algal pigment data
51 obtained exclusively by High-Performance Liquid Chromatography (HPLC), containing
52 10,798 samples collected across 77 Arctic research cruises between 2000 and 2024. As
53 a result of large-scale collaborative effort, this database covers both open water and
54 sea-ice environments across coastal, shelf and open domains. The database
55 (<https://doi.org/10.11583/DTU.29445104>) includes measures of up to 26 pigments, with
56 8 major marker/accessory pigments being considered in this study, namely Alloxanthin
57 (Allo), 19'-Butanoyloxyfucoxanthin (But-fuco), Chlorophyll a (Chl-a), Chlorophyll b (Chl-
58 b), Fucoxanthin (Fuco), 19'-Hexanoyloxyfucoxanthin (Hex-fuco), Peridinin (Peri), and
59 Zeaxanthin (Zea) (Heidemann et al., 2026). This publicly available database provides
60 crucial data that can be used to assess phytoplankton dynamics, validating remote
61 sensing observations and can serve as a resource for future Arctic ecological- and
62 modelling studies.

63

64

65



66 1. Introduction

67 Climate change has disproportionately affected the Arctic, shown by drastic increases
68 in temperature and ongoing sea-ice decline (England et al., 2021; Stroeve and Notz,
69 2018). Changing conditions in the Arctic have already altered the food web, with studies
70 indicating further impacts in the near future (Ardyna and Arrigo, 2020; Arrigo and van
71 Dijken, 2015; Flores et al., 2023; Freer et al., 2022; Quinlan et al., 2005). As the
72 foundation of marine food webs, phytoplankton and sea-ice algae are critical for
73 sustaining ecosystems and contribute to large parts of global primary production,
74 leading to energy transfer across trophic levels and ultimately carbon sequestration
75 (Falkowski, 1994; Serra-Pompei et al., 2022). Environmental heterogeneity and changes
76 may alter community composition, with the potential to impact large-scale ecological
77 processes. For example, in the Arctic and sub-Arctic regions, increased open water
78 areas has led to a longer phytoplankton growing season likely associated with changes
79 in community composition. Studies have demonstrated that climate change may favor
80 increased biomass of smaller flagellated phytoplankton species, leading to reduced
81 dominance of large diatoms species (Blais et al., 2017; Coupel et al., 2012; Vonnahme
82 et al., 2025). This can impact the structure of the food web and overall carbon cycling by
83 having an immediate effect on higher trophic levels, potentially influencing the
84 abundance, distribution and feeding preferences of zooplankton (Campbell et al., 2009;
85 Negrete-García et al., 2024).

86 Characterising phytoplankton community composition is therefore essential for better
87 understanding ecosystem structure, dynamics and services, especially in the under-
88 sampled Arctic seas, which have experienced the greatest impact of climate change in
89 recent years (England et al., 2021). It is clear that long-term data on microalgae
90 physiology and biomass are vital to enhance our ability to assess and detect spatial and
91 temporal patterns in phytoplankton and sea-ice algae community structure and
92 physiology in response to environmental change. Many studies have used pigment-
93 based measurements, but datasets are often scattered across many sources. This
94 makes it difficult to obtain, access and synthesize into a larger spatial and temporal
95 scale. To address this gap, our paper provides baseline information regarding
96 phytoplankton and sea-ice algae biomass and photosynthetic pigments in the Arctic
97 Ocean aiming at providing a framework to support such large-scale Arctic algae studies
98 across two decades of data.

99 Phytoplankton pigments, particularly chlorophyll a (Chl-a), drives photosynthesis by
100 harvesting light and protecting the cells (Pereira and Gonçalves, 2022). Advances in
101 pigments analysis through High-Performance Liquid Chromatography (HPLC) and ultra
102 HPLC (UHPLC), have enabled precise identification and quantification of a suite of
103 photosynthetic and photoprotective microalgal pigments. These pigments can serve as
104 chemotaxonomic markers for major functional and taxonomic phytoplankton groups,



105 including the commonly used diagnostic pigments, Alloxanthin (Allo), 19'-
106 Butanoyloxyfucoxanthin (But-fuco), Chlorophyll b (Chl-b), Fucoxanthin (Fuco), 19'-
107 Hexanoyloxyfucoxanthin (Hex-fuco), Peridinin (Peri), and Zeaxanthin (Zea) used in this
108 study. Additionally and when available, the database presented in this paper also
109 includes α - β -carotene ($\alpha\beta$ -Car), Bacteriochlorophyll a, Chlorophyllide a (Chlide a), Chl-
110 c1, Chl-c1+c2, Chl-c3, Diadinoxanthin (Diadino), Diatoxanthin (Diato), Divinyl
111 Chlorophyll a and b (DV-Chl-a and DV-Chl-b), Lutein (Lut), Neoxanthin (Neo),
112 Pheophorbide a (Phide a), Pheophytin a (Phytin a), Prasinoxanthin (Pras) and
113 Violaxanthin (Viola) (Jeffrey et al., 1999) (**Table 1**). These additional accessory pigments
114 can be used by phytoplankton to adapt and/or acclimate to various light regime
115 changes that occur in the environment (Brunet et al., 2011). Variability in pigment
116 composition can reflect strategies such as photoprotection, which involves the
117 production of pigments that mitigate damage from excessive light and photo
118 acclimation that refers to the ability of algae to adjust their pigment composition in
119 response to light intensity changes that hereby can optimise photosynthetic efficiency
120 (Bonilla et al., 2009; Gosselin et al., 2017).

121 Absorption and scattering of light by phytoplankton pigments and other cellular
122 constituents allow their detection by radiometers, making them an invaluable source
123 for remote sensing applications (see overview in Bracher et al., 2017). Multispectral
124 satellite sensors such as SeaWiFS, MODIS, MERIS and OLCI have paved the way and
125 demonstrated the ability to distinguish phytoplankton functional types on large scales
126 (Miller, 2004; Nieke et al., 2015). Recent development have focused on hyperspectral
127 sensors, capable of measuring more narrow absorption and reflectance properties, that
128 can be missed by multispectral sensors (Hu, 2022). Successful applications include
129 ENVISAT's Scanning Imaging Absorption Spectrometer for Atmospheric Cartography
130 (SCIAMACHY) using the PhytoDOAS method (Bracher et al., 2009; Sadeghi et al., 2012)
131 and the DLR Earth Sensing Imaging Spectrometer Mission (DESI) using the
132 WebAssembly System Interface (WASI) (Gege, 2004, 2014) by (Bracher et al., 2021).
133 Most recently NASA's Plankton, Aerosol, Clouds, ocean Ecosystem (PACE) mission have
134 been launched (Werdell et al., 2024) and the European Space Agency (ESA) is preparing
135 the CHIME hyperspectral to be launched in the coming decade (Nieke et al., 2023).

136 Since satellites provide long-term synoptic observations of phytoplankton groups high-
137 quality in situ pigment data is invaluable for product validation and algorithm
138 refinement (Cetinić et al., 2024). Similarly, several studies based on self-organizing
139 maps, spectral composition or machine-learning-based methods applied to satellite
140 data have leveraged phytoplankton pigments to understand taxonomic shifts in
141 phytoplankton communities (El Hourany et al., 2019, 2024; Hayward et al., 2025; Xi et
142 al., 2020).



143 **Table 1.** Alphabetically ordered list of the major diagnostic pigments and additional accessory pigments considered
 144 in this study (including abbreviations, their full name and associated phytoplankton groups) (Fragoso et al., 2017;
 145 Jeffrey et al., 1999).

Major diagnostic pigments		
Abbreviation	Pigment name	Associated phytoplankton groups
Allo	Alloxanthin	Cryptophytes
But-fuco	19'-Butanoyloxyfucoxanthin	Haptophytes, Pelagophytes
Chl- <i>a</i>	Chlorophyll <i>a</i>	All phytoplankton groups
Chl- <i>b</i>	Chlorophyll <i>b</i>	Green algae (chlorophytes and prasinophytes)
Fuco	Fucoxanthin	Diatoms, Pelagophytes, Dinoflagellates-2, Haptophytes (certain species of <i>Phaeocystis</i>)
Hex-fuco	19'-Hexanoyloxyfucoxanthin	Haptophytes, Dinoflagellates-2
Peri	Peridinin	Dinoflagellates-1
Zea	Zeaxanthin	Cyanobacteria, Green algae
Additional accessory pigments		
Abbreviation	Pigment name	
$\alpha\beta$ -Car	α - β -carotene	
Bacteriochlorophyll <i>a</i>	Bacteriochlorophyll <i>a</i>	
Chlide <i>a</i>	Chlorophyllide <i>a</i>	
Chl-c1	Chlorophyll c1	
Chl-c1+c2	Chlorophyll c1+c2	
Chl-c3	Chlorophyll c3	
Diadino	Diadinoxanthin	
Diato	Diatoxanthin	
DV-Chl- <i>a</i>	Divinyl Chlorophyll <i>a</i>	
DV-Chl- <i>b</i>	Divinyl Chlorophyll <i>b</i>	
Lut	Lutein	
Neo	Neoxanthin	
Phide <i>a</i>	Pheophorbide <i>a</i>	
Phytin <i>a</i>	Pheophytin <i>a</i>	



Pras	Prasinoxanthin
Viola	Violaxanthin

146

147 While satellite data are becoming increasingly important, it remains limited by its ability
148 to capture only the first optical depth under cloud- and ice-free conditions.

149 In situ pigment data from the Arctic have compared to other parts of the world
150 historically been limited due to the region's remoteness, harsh weather conditions and
151 logistical challenges of conducting fieldwork in such remote regions. Advances in HPLC
152 technology, together with standardised protocols (Hooker et al., 2005) and round-robins
153 intercomparison of methodologies (Canuti, 2023), have contributed to the growing
154 availability of pigment data globally, which also includes data from the Arctic and Sub-
155 arctic regions (Hayward et al., 2024; Kramer et al., 2022; Losa et al., 2017; Mattei and
156 Scardi, 2021; Swan et al., 2016; Xi et al., 2023). Related efforts to obtain pigment data,
157 such as those using UPLC methods (Hwang, 2025), also represent a valuable
158 contribution, though they cannot be incorporated into the current database for inter-
159 comparability reasons with HPLC-based measurements. Despite advances, spatial and
160 temporal coverage across the Arctic remains uneven, underscoring persistent
161 knowledge gaps, highlighting the need for coordinated, collective efforts to compile and
162 expand existing data in this rapidly changing region.

163 To address this gap, we present the first pan-Arctic overview of phytoplankton and sea-
164 ice algae pigment distributions, based on a comprehensive database of Arctic and sub-
165 Arctic in situ pigment measurements collected between 2000 and 2024. The database
166 is compiled from 77 cruises conducted across the Arctic Ocean, covering coastal,
167 shelf, open-ocean and sea-ice domains (see **Table 2**). Importantly, this database
168 represents a collective effort involving multiple institutions, research teams and
169 international collaborations. By consolidating data from diverse sources, it provides a
170 baseline for assessing long-term trends in phytoplankton pigments, communities and
171 their ecological responses to environmental change. Additionally, such a database can
172 support a pan-Arctic taxonomic characterisation of phytoplankton communities by
173 employing pigment-based taxonomy techniques (Hayward et al., 2023, 2024; Vidussi et
174 al., 2001; Wright and Jeffrey, 2006).

175

176



177 Methodology

178 2.1. Database Compilation

179 Phytoplankton and ice algae pigment data was compiled from 77 research cruises
 180 conducted between 2000 and 2024. The datasets were sourced from a combination of
 181 publicly available repositories (e.g., PANGAEA), institutional databases (e.g., NASA) and
 182 personal correspondence with scientists. Datasets were accompanied by relevant
 183 ancillary metadata, including information on sampling time, location and depth. A total
 184 of 10,798 pigment datapoints were compiled (**Table 2**). Where possible, cruise reports
 185 and original publications were consulted to verify the context and methods of data
 186 collection. Part of the data has already been published individually for the respective
 187 research cruises and/or projects, however, the compiled database presented in this
 188 article (including datasets not yet publicly available) has been stored in a public
 189 repository (<https://doi.org/10.11583/DTU.29445104>).

190 **Table 2.** Alphabetically ordered summary of Arctic and sub-Arctic cruises (= 77) with key dataset information such as
 191 year, sampling region(s) (as defined in section 3.1.), environment, sample count and associated DOI, where possible.
 192 Note that few samples were from melt-ponds, here assigned as ice samples.

Dataset	Year	Region(s)	Environment(s)	Number of Samples	DOI
ARA06B	2015	North Pacific Ocean, East Siberian Sea, Chukchi Sea, CAO	Water	112	https://dx.doi.org/doi:10.22663/KOPRI-KPDC-00002844
ARA07B	2016	North Pacific Ocean, East Siberian Sea, Chukchi Sea	Water	50	
ARA08B	2017	North Pacific Ocean, East Siberian Sea, Chukchi Sea	Water	98	
ARA09B	2018	East Siberian Sea, Chukchi Sea	Water	110	
ARA10B	2019	North Pacific Ocean, East Siberian Sea, Chukchi Sea	Water	70	
ARA10B_Ice	2018	East Siberian Sea	Ice	65	
ARA11B	2020	North Pacific Ocean, East Siberian Sea, Chukchi Sea	Water	85	
AREX2000	2000	Norwegian Sea, Barents Sea, Fram Strait	Water	77	https://doi.org/10.48457/IOPAN.2025.523
AREX2001	2001	Norwegian Sea, Barents Sea, Fram Strait	Water	55	
AREX2002	2002	Norwegian Sea, Fram Strait	Water	20	



AREX2003	2003	Norwegian Sea, Barents Sea, Fram Strait	Water	50	
AREX2004	2004	Norwegian Sea, Fram Strait	Water	27	
AREX2005	2005	Norwegian Sea, Barents Sea, CAO, Fram Strait	Water	51	
AREX2014	2014	Norwegian Sea, Barents Sea, CAO, Fram Strait	Water	133	
AREX2019	2019	Barents Sea, CAO, Fram Strait	Water	113	
AREX2021	2021	Norwegian Sea, Barents Sea, Fram Strait	Water	59	
AREX2022	2022	Norwegian Sea, Barents Sea, CAO, Fram Strait	Water	140	
Academik_loffe_2003	2003	Greenland Sea, Labrador Sea, Norwegian Sea	Water	34	
Arc2002	2002	Beaufort Sea, Chukchi Sea	Water	53	
Arc2004	2004	Beaufort Sea, Chukchi Sea	Water	90	
Arctic_Ocean_2024	2024	CAO	Ice, Water	61	https://doi.org/10.48457/IOPAN.2025.386
Arex2017	2017	CAO, Fram Strait	Water	33	
Assmy_ICE2010	2010	CAO	Water	42	
BODC/NERC_2001	2001	Greenland Sea	Water	169	http://doi.pangaea.de/10.1594/PANGAEA.793246
BODC/NERC_2002	2002			419	
BaySys	2018	Hudson Bay, Labrador Sea	Ice, Water	131	https://canwin-datahub.ad.umanitoba.ca/data/dataset/algal-pigments-icewater
Bracher2021_PS126	2021	Norwegian Sea, Fram Strait	Water	175	https://doi.pangaea.de/10.1594/PANGAEA.982954
Bracher_2017_PS106	2017	Norwegian Sea, Barents Sea, CAO, Fram Strait	Ice, Water	40	https://doi.org/10.1594/PANGAEA.899284
Bracher_2019_PS121	2019	Norwegian Sea, Fram Strait	Water	298	https://doi.org/10.1594/PANGAEA.941011
Bracher_2020_MSM93	2020	Norwegian Sea, Greenland Sea, Fram Strait	Water	219	
Bracher_2022_PS131_ATWAICE	2022	Norwegian Sea, Greenland Sea, CAO, Fram Strait	Water	241	https://doi.pangaea.de/10.1594/PANGAEA.983242
Bracher_2023_PS136_HAUSGARTEN	2023	Norwegian Sea, Fram Strait	Water	137	https://doi.pangaea.de/10.1594/PANGAEA.983243



Bracher_2024_PS143.2	2024	Norwegian Sea, CAO, Fram Strait	Water	212	https://doi.pangaea.de/10.1594/PANGAEA.983244
CFL	2008	Beaufort Sea, Canadian Archipelago	Water	75	
DANA_ECOTIP_2021	2021	Baffin Bay, Labrador Sea	Water	16	https://doi.org/10.48457/IOPAN.2025.523
DSOS_GINR	2024	Baffin Bay, Labrador Sea	Water	234	
DiTuillio_2018	2018	CAO	Water	132	10.18739/A2028PD2H
Fragoso_2005	2005	Labrador Sea	Water	25	https://doi.pangaea.de/10.1594/PANGAEA.871872
Fragoso_2006	2006	Labrador Sea	Water	12	
Fragoso_2007	2007	Labrador Sea	Water	32	
Fragoso_2008	2008	Labrador Sea	Water	25	
Fragoso_2009	2009	Labrador Sea	Water	26	
Fragoso_2010	2010	Labrador Sea	Water	27	
Fragoso_2011	2011	Labrador Sea	Water	33	
Fragoso_2012	2012	Labrador Sea	Water	30	
Fragoso_2013	2013	Labrador Sea	Water	27	
Fragoso_2014	2014	Greenland Sea, Labrador Sea	Water	16	
GreenEdge_Amundsen	2016	Baffin Bay, Labrador Sea	Water	589	10.17882/86417
Icescape_2010	2010	Chukchi Sea	Water	100	https://seabass.gsfc.nasa.gov/experiment/ICESCAPE
Icescape_2011	2011	Beaufort Sea, Chukchi Sea	Water	455	
Liu2015_PS93.2	2015	Norwegian Sea, Fram Strait	Water	241	
Liu_2016_PS99.1	2016	Norwegian Sea, Fram Strait	Water	96	https://doi.pangaea.de/10.1594/PANGAEA.905502
Liu_2016_PS99.2	2016	Fram Strait	Water	230	https://doi.pangaea.de/10.1594/PANGAEA.894874
Liu_2017_PS107	2017	Norwegian Sea, Fram Strait	Water	262	https://doi.pangaea.de/10.1594/PANGAEA.894860
MERIAN_ECOTIP2022	2022	Greenland Sea, Fram Strait	Water	40	https://doi.org/10.48457/IOPAN.2025.523
MOSAIC_Algal	2019, 2020	CAO, Fram Strait	Ice, Water	260	FYI samples: https://doi.pangaea.de/10.1594/PANGAEA.967448
MOSAIC_SYI	2019, 2020	CAO	Ice	275	
MOSAIC_FYI	2019, 2020	CAO, Fram Strait	Ice	285	SYI samples: https://doi.pangaea.de/10.1594/PANGAEA.967450 Open water samples: https://doi.org/10.1594/PANGAEA.955763
MR17-05	2017	Beaufort Sea, North Pacific Ocean, Chukchi Sea	Ice, Water	74	https://www.godac.jamstec.go.jp/darwin_cruise/view/metadata?key=MR17-05C&lang=en
Malina	2009	Baffin Bay, Labrador Sea, Beaufort Sea, Canadian Archipelago, Laptev Sea, North Pacific Ocean, Chukchi Sea	Water	677	
Malina_Barge	2009	Beaufort Sea	Water	53	https://www.seanoe.org/data/00641/75345/



N-ICE2015	2015	CAO	Water	145	https://doi.org/10.21334/NPOLAR.2016.3EBB7F64
NunaWP4Mackenzie	2019	Beaufort Sea	Water	140	https://doi.org/10.1594/PANGAEA.937585
Thielecke_PS138_Arc Watch	2023	CAO	Ice, Water	151	
Peeken, PS74	2009	Norwegian Sea, Greenland Sea, Fram Strait	Water	130	
Peeken, PS76	2010	Norwegian Sea, Greenland Sea, Fram Strait	Water	549	
Peeken, PS78	2011	Fram Strait	Water	264	
Peeken, PS80	2012	Laptev Sea, CAO, Fram Strait	Water	576	
Peeken, PS85	2014	Fram Strait	Water	82	
Peeken, PS92	2015	CAO	Water	106	
Polarstern2003	2003	Greenland Sea, Norwegian Sea	Water	26	https://doi.org/10.48457/IOPAN.2025.523
SeaBASS_2004	2004	Beaufort Sea, Chukchi Sea	Water	59	
SeaBASS_2008	2008	Greenland Sea	Water	43	
SeaBASS_2013	2013	Baffin Bay, Labrador Sea, Norwegian Sea, Beaufort Sea, Barents Sea, East Siberian Sea, Canadian Archipelago, Chukchi Sea, Greenland Sea, Kara Sea	Water	77	
SubIce	2014	Chukchi Sea	Water	155	
Tara_Arctic	2013	Baffin Bay, Labrador Sea, Norwegian Sea, East Siberian Sea, Barents Sea, Canadian Archipelago, Greenland Sea, Kara Sea	Water	229	
Woodfjorden	2024	Fram Strait	Water	50	https://doi.org/10.48457/IOPAN.2025.504

193

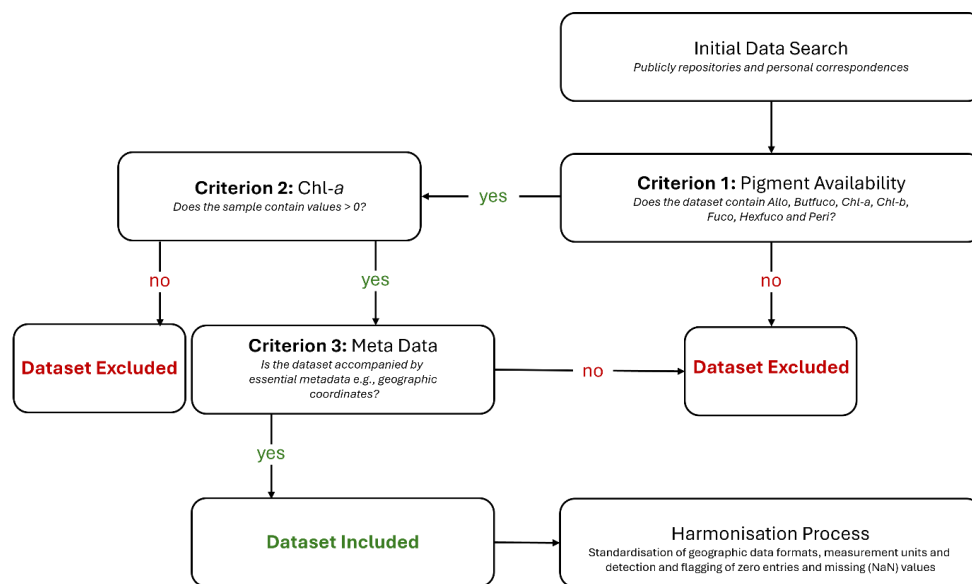
194 2.2. Data Quality Measures

195 This dataset integrated HPLC pigment measurements from 77 research cruises, each
 196 carried out by laboratories using their own established laboratory procedures, including
 197 different HPLC set-ups, calibration standards and water filtration volume.



198 Methodological descriptions associated with each dataset can be accessed through
199 the provided DOIs in **Table 2** or by contacting the original data providers. To ensure
200 consistency and comparability across sources, we applied a set of inclusion/exclusion
201 criteria and harmonisation procedures to ensure data consistency and comparability
202 across sources. Only datasets with measurements of seven out of the eight marker
203 pigments described in **Table 1** were included in the database, allowing for reliable inter-
204 sample comparison of pigment composition (criterion 1, see **Figure 1**). Although
205 zeaxanthin is normally included in the analysis of phytoplankton functional types, it was
206 excluded as a formal requirement in this database compilation because one source
207 lacked measurement of this pigment and reliable distinction of green algae from other
208 phytoplankton groups remain possible without zeaxanthin (see available pigments for
209 each cruise in Supplementary **S1**). Zeaxanthin is also a major diagnostic pigment for
210 *Synechococcus*, which is largely absent from the Arctic region due to its thermal
211 dependence on warmer waters (Six et al., 2021). Samples were excluded from the final
212 database if they reported Chlorophyll (Chl-*a*) concentration of zero (criterion 2, see
213 **Figure 1**), lacked measurements of the required marker pigments and/or were missing
214 essential metadata such as geographic coordinates (criterion 3, see **Figure 1**).

215



216

217 **Figure 1.** Workflow diagram displaying the major decisions in the data compilation process.

218 In addition to data filtering, multiple data harmonisation steps were also undertaken:
219 longitudes reported in degrees East (0° to 360°E) were converted to signed longitude (-
220 180° to 180°E/W) to ensure spatial compatibility with standard mapping tools ; datasets
221 were also checked for true 0s and NaNs and that the distinction between these were



222 standardised across datasets. This process required manual inspection of each
223 dataset: If a pigment was entirely absent from a dataset, it was treated as NaNs (empty
224 cells), whereas if a pigment was present but only had a single non-zero value reported,
225 the remaining empty cells were interpreted as true 0s; finally, concentration units for
226 accessory pigments and Chl-*a* were also standardised to the common unit, $\mu\text{g/L}$.
227 Considerable variability in methods used to calculate total Chl-*a* was observed across
228 the database, or were not reported. This parameter was therefore excluded. In addition,
229 a limited number of melt pond samples were available. These were treated as part of
230 the ice sample category.

231

232 2.3. Limitations and Uncertainties of the Dataset

233 Despite efforts to minimize both limitations and uncertainties, this dataset consists of
234 HPLC measurements from multiple laboratories. We acknowledge that methodological
235 variability between laboratories exists and will introduce variability to the dataset. The
236 following sections are provided to summarise the main known sources of limitations
237 and uncertainties associated with compiling HPLC data from various laboratories, as
238 well as general uncertainties inherent to pigments measurements.

239

240 *Analytical*

241 All datasets presented in this paper have followed standard protocols for HPLC analysis
242 of phytoplankton pigments. However, analytical uncertainties can arise from multiple
243 stages of the workflow. As outlined by Wright & Jeffrey (2006), these can broadly be
244 categorised into:

- 245 • **Collection and storage**
246 Filtration volume, filter type and size, storage temperature and storage time
- 247 • **Extraction procedures**
248 Sample disruption and choice of solvents
- 249 • **HPLC methods and techniques** (see review of HPLC pigment methods in Roy et
250 al., 2011)
251 Variations of column type and flow rate etc.
- 252 • **Peak detection, identification, integration and quantification**
253 Differences in baseline correction, peak threshold, co-elution handling and
254 pigment standards used for calibration

255 To minimize bias in each of these steps, substantial effort has been made through inter-
256 comparability studies. Most notably are the SeaWiFS HPLC Analysis Round-Robin
257 Experiments (SeaHarre-1 to SeaHarre-5) (Hooker et al., 2012) and HPLC/DAD
258 intercomparison on phytoplankton pigments (HIP-1 to HIP-4) (Artuso, F et al., 2016;



259 Canuti et al., 2016), which efforts has been to eliminate differences in pigment
260 quantification across laboratories and quantify these uncertainties in terms of what can
261 be expected, even when conducting analysis according to strict protocols.

262

263 *Pigment-Specific*

264 In addition to the analytical sources of uncertainties, pigment-specific sources also
265 exist because of a varying degree of sensitivity to the above-described workflow. Any
266 chosen HPLC method can therefore increase or reduce the variance experienced for a
267 specific pigment. However, defining robust “uncertainty values” for each individual
268 pigment remains a challenge across analytical methods. Recent inter-laboratory
269 comparisons highlight this challenge, while also underscoring the need of such
270 estimates in applications such as remote sensing validation (e.g., Canuti, 2023).

271 A main source of pigment-specific behavior comes from differences in the chemical
272 stability of the pigments. This will affect their susceptibility to degradation, co-elution
273 and extraction efficiency. For example, Chlorophylls (a, b, c₁ and c₂) are prone to
274 degradation, particularly during storage and extraction, producing degradation products
275 such as pheophytins and chlorophyllides. This can lead to biased and unprecise
276 chlorophyll estimations as well as co-elution issues. This have often been reported for
277 chlorophyll c₁ and chlorophyll c₂ as well as for the Fuco derivatives (But-fuco and Hex-
278 fuco) (Roy et al., 2011; Simmons et al., 2016; Wright and Jeffrey, 2006; Zapata et al.,
279 2000). Additionally, some chlorophyll degradation products, for example Phide *a* and
280 Phytin *a*, can co-elute with carotenoids due to polarity changes (Mendes et al., 2007).

281 Finally, pigment concentration itself can be a major source of uncertainty. This is
282 particularly true for low-abundance accessory pigments, which often approach the
283 instrumental limits of detection (LOD) (Bidigare et al., 2002; Canuti, 2023; Canuti et al.,
284 2016; Claustre et al., 2004; Hooker et al., 2005). For instance, when pigment
285 concentrations fall below 0.01 mg m⁻³, the relative standard deviation can reach up to
286 nearly double that of pigments present at higher concentrations (Claustre et al., 2004).

287

288

289

290

291

292



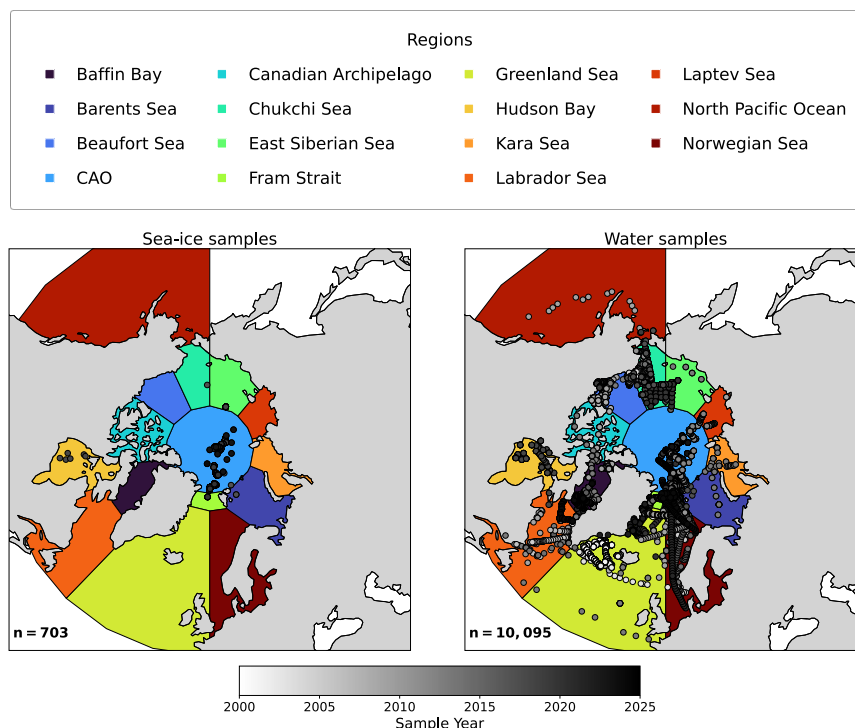
293 3. Data Description

294

295 3.1. Sampling Coverage

296 To classify the sampling efforts across the Arctic and sub-Arctic seas into common
297 groups, the study area was subdivided into 14 regions (**Figure 2**). A total of 10,095 water
298 samples and 703 sea-ice samples were compiled and mapped according to their
299 geographic location. Water samples displayed extensive sampling across most regions,
300 while ice samples were comparatively sparse and primarily concentrated in the Central
301 Arctic Ocean (CAO), Canadian Archipelago and Hudson Bay. These samples originate
302 from a limited number of cruises and are not consistently represented throughout the
303 years. Regional sampling frequencies are summarised in **Figure 2**, highlighting the
304 dominance of water samples and the uneven spatial distribution of sea-ice samples.

305



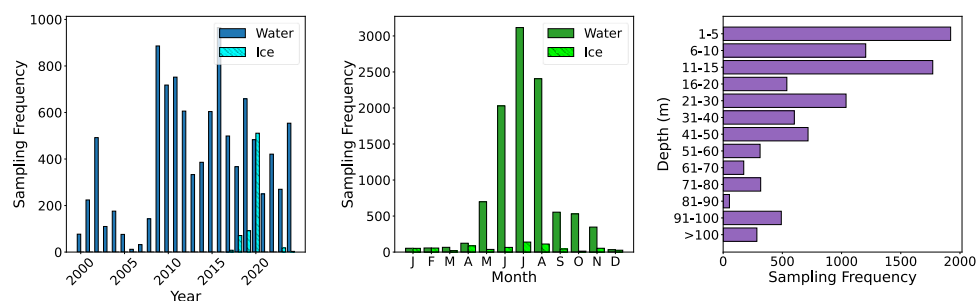
306

307 **Figure 2.** Map showing the spatial distribution of water and sea-ice samples across 14 defined regions of the Arctic
308 and sub-Arctic seas. Each point represents an individual sampling location and is colored according to the year of
309 collection.

310 Overall, the water sample collection also varied substantially across years, with higher
311 coverage in 2002, 2009, 2016 and 2020 (**Figure 3**). These periods correspond to large-



312 scale, multidisciplinary campaigns such as MALINA (Coupel et al., 2015), GreenEdge
313 (Bruyant et al., 2022; Massicotte et al., 2020), the AR7W transect during the MOSAiC
314 cruise and others, including global initiatives such as the International Polar Year (IPY).
315 Additionally, the MAREDAT pigment database represents a major synthesis effort
316 (Peloquin et al., 2013) (see **Table 1**).



317

318 **Figure 3.** (Left) yearly sampling frequency for water column and sea-ice samples, (middle) monthly sampling
319 frequency and (right) number of water samples observations per depth bin. Note that for sea-ice samples, the vertical
320 distribution is not presented due to inconsistencies in the ice core sampling methods among the different campaigns.

321 Seasonally, sampling frequency was the highest in spring and summer (May-August).
322 Sampling frequency was lower in September, followed by a notable secondary drop in
323 December. The lowest sampling frequency is observed during winter and early spring
324 (December-March), when there is extensive sea ice extent. Sampling frequency also
325 varied vertically in the water column (**Figure 3**). Most samples were collected within the
326 upper 1-15 meters range. Sampling frequency consistently declines from 21-30 meters
327 onward, before a slight increase in the 91-100 meters range.

328

329 3.2. Pigment Distribution

330 Pigment concentration in water and sea-ice samples exhibited considerable variability
331 in the biomass and composition of algal communities as well as in the spatiotemporal
332 structure of the database (**Table 3**). In addition, the observed variability can also be
333 attributed to adaptive pigment strategies.

334 Since direct comparison of absolute pigments concentrations between sea-ice and
335 water samples should be interpreted with caution, only a brief description of absolute
336 pigment concentration is provided for context (**Table 3a**). Chl-*a*, the primary indicator of
337 phytoplankton and sea-ice algae biomass, had a mean concentration of 0.997 $\mu\text{g/L}$ in
338 water samples and 0.639 $\mu\text{g/L}$ in sea-ice samples although the highest individual values
339 in both environments point to episodic blooms. The highest concentration across the
340 database, 32.76 $\mu\text{g/L}$, was recorded in the Chukchi Sea originating from the Ice Scape
341 dataset in August 2010. In general, such high concentrations are rare, with the majority
342 of samples falling below 0.5 $\mu\text{g/L}$ across seasons. Overall, concentrations were highly



343 variable with 90% of values falling between 0.017 and 3.789 $\mu\text{g/L}$ in water samples and
 344 between 0.022 and 0.292 $\mu\text{g/L}$ in sea-ice samples (**Table 3a**). It should be recognised
 345 that there is a potential bias when comparing open-water and bulk-ice samples due to
 346 neglect of the dilution of pigments from sympagic algae (Chamberlain et al., 2022;
 347 Gradinger, 2009; Miller et al., 2015).

348 In terms of the relative ratios to Chl-*a* (**Table 3b and Figure 4**) the database also showed
 349 marked seasonal variability. Among the eight analysed marker pigments, Fuco
 350 consistently had the highest ratios, particularly during winter months, followed by a
 351 decline through summer and early autumn. The Fuco-derivatives, But-fuco and Hex-
 352 fuco, both considered diagnostic markers of haptophytes, had a stable distribution
 353 throughout the year, aside from notable peaks in November. Additionally, Hex-fuco had
 354 a higher overall proportion than But-fuco, implying higher proportion of dinoflagellates.

355 The ratio of Allo, a distinct marker pigment of cryptophytes, started to increase in late
 356 winter, prior to the main growing season. Perid, which is a marker pigment of
 357 dinoflagellates, had low overall ratios. These ratios increased during summer, peaking in
 358 October, before they exhibited a sharp decline toward the onset of December. As
 359 expected, Zea and Chl-*b* were relatively aligned throughout most of the year, consistent
 360 with their shared role as a marker pigment of green algae. However, a marked
 361 dissimilarity in their patterns occurred in November, when Chl-*b* declined while Zea
 362 increased.

363 For the sea-ice samples, the only accessory pigments with high ratios are Fuco and Chl-
 364 *b*.

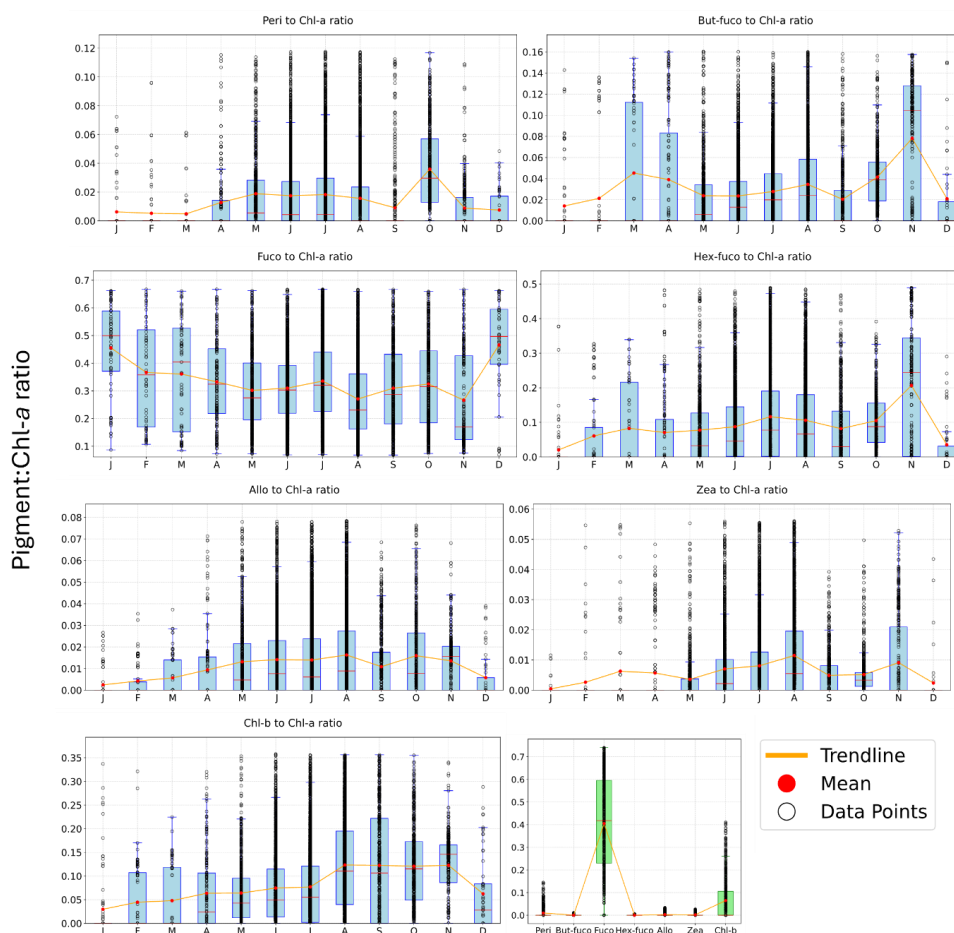
365 These differences suggest distinct pigment signatures between sea-ice and water
 366 samples, underscoring the importance of expanding sea-ice sampling efforts to better
 367 capture algae dynamics in this environment.

368 **Table 3.** Summary of 5th, 95th, mean, median and std statistics across all cruises (= 77), for (a) pigment concentration
 369 categorized by sample type and (b) relative ratio of accessory pigments vs. Chl-*a*, For detailed pigment information by
 370 individual cruises, see Supplementary **Table S1**. For detailed information about all pigments across environments,
 371 see Appendices **Table A1**

(a)	Water Samples ($\mu\text{g/L}$)					Sea-ice Samples ($\mu\text{g/L}$)				
	5 th percentile	95 th percentile	Mean	Median	Std	5 th percentile	95 th percentile	Mean	Median	Std
Allo	0.000	0.061	0.014	0.003	0.031	0.000	0.016	0.004	0.000	0.020
But-fuco	0.000	0.080	0.020	0.007	0.040	0.000	0.005	0.001	0.000	0.008
Chl- <i>a</i>	0.017	3.789	0.997	0.417	1.855	0.022	2.292	0.639	0.179	1.746
Chl- <i>b</i>	0.000	0.207	0.059	0.033	0.091	0.000	0.158	0.037	0.000	0.109



Fuco	0.003	1.493	0.357	0.106	0.853	0.000	1.392	0.367	0.063	1.120
Hex-fuco	0.000	0.434	0.092	0.019	0.180	0.000	0.011	0.002	0.000	0.010
Peri	0.000	0.105	0.021	0.001	0.072	0.000	0.057	0.016	0.000	0.078
Zea	0.000	0.030	0.008	0.001	0.025	0.000	0.009	0.003	0.000	0.022
(b)	Water Samples (ratio)					Sea-ice Samples (ratio)				
Parameter / Pigment	5 th percentile	95 th percentile	Mean	Median	Std	5 th percentile	95 th percentile	Mean	Median	Std
Allo vs Chl- <i>a</i>	0.000	0.078	0.100	0.009	1.634	0.000	0.034	0.006	0.000	0.021
But-fuco vs Chl- <i>a</i>	0.000	0.160	0.263	0.024	4.663	0.000	0.013	0.003	0.000	0.030
Chl- <i>b</i> vs Chl- <i>a</i>	0.000	0.358	1.094	0.077	15.482	0.000	0.414	0.087	0.000	0.138
Fuco vs Chl- <i>a</i>	0.068	0.666	2.504	0.290	26.620	0.000	0.741	0.428	0.443	0.235
Hex-fuco vs Chl- <i>a</i>	0.000	0.489	0.681	0.080	9.694	0.000	0.007	0.004	0.000	0.018
Peri vs Chl- <i>a</i>	0.000	0.118	0.221	0.004	5.792	0.000	0.150	0.028	0.000	0.109
Zea vs Chl- <i>a</i>	0.000	0.056	0.056	0.003	1.062	0.000	0.027	0.005	0.000	0.021



373

374 **Figure 4.** Display of the seasonal variation of individual accessory pigment concentration to Chl-a ratio. Water
 375 samples are shown as monthly ratios in blue and sea-ice samples are shown overall across months per pigment in
 376 green. Only values within 5th to 95th percentile are included. Data points are displayed as open circles, the mean ratio
 377 for each month is shown as a red dot and an orange line connects means.

378

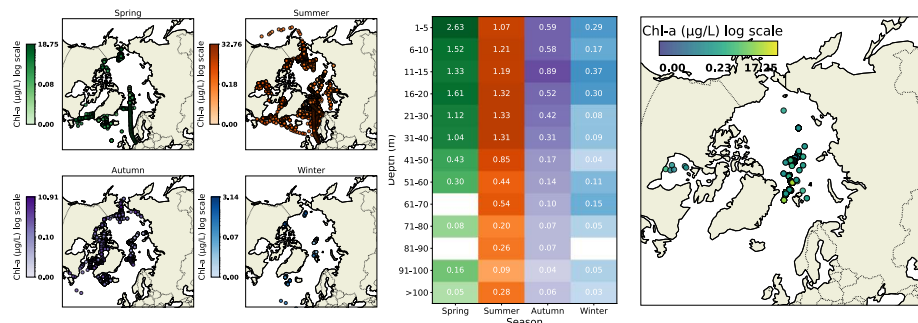
379 *Spatial and Temporal Dynamics*

380

381 In our dataset, Chl-a exhibited strong spatial and temporal (seasonal) and inter-annual
 382 variability, reflecting the dynamic nature of phytoplankton and sea-ice algae in polar
 383 and subpolar environments. Elevated concentrations were observed in areas such as
 384 the Fram Strait, Barents Sea, Beaufort Sea, Chukchi Sea and Labrador Sea (**Figure 5**).
 385 However, as the database is opportunistic by nature, covering only discrete regional
 386 samplings, spatial and seasonal comparisons should be made with caution.



387 In spring, the Labrador Sea recorded the seasonal maximum (18.75 $\mu\text{g/L}$), with the
388 highest values occurring mostly in surface waters (0-5 meters). As previously
389 mentioned, summer exhibited the maximum database record for Chl-*a*. Contrary to
390 spring, highest averages were found between 16-30 meters. By autumn, Chl-*a* had
391 declined across most regions. However, localised high biomass persisted in some areas
392 such as Beaufort Sea, Chukchi Sea and Fram Strait. Winter Chl-*a* was generally low.
393

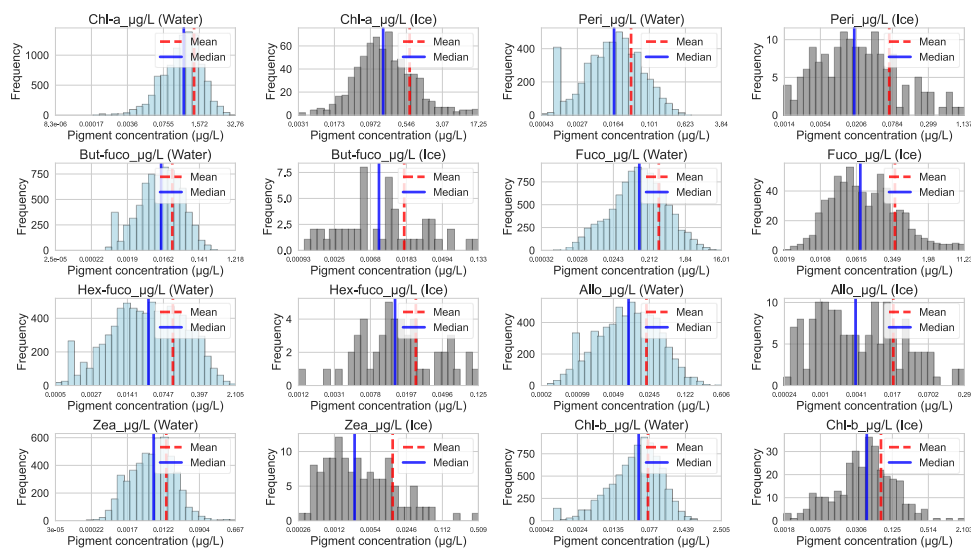


394

395 **Figure 5.** (a) Spatial distribution of all measured Chl-*a* water samples in each season, shown as subplots for spring,
396 summer, autumn and winter. Color mapping uses logarithmic scale, but the values themselves are not log-
397 transformed. (b) Mean Chl-*a* concentration as function of depth range (rows) and season (columns). Color indicates
398 the average value for each depth/season bin. Missing color indicates that data is not available. (c) Spatial distribution
399 of all measured Chl-*a* for sea-ice samples.

400

401 The concentration frequency distribution plots of water samples (**Figure 6**, blue plots)
402 showed that both Chl-*a*, Chl-*b* and Fuco exhibited approximately log-normal
403 distribution, with peak concentrations near central values and tails on either side. This
404 interpretation was supported by the log-normal distribution of data. However, formal
405 normality tests such as Kolmogorov-Smirnov (K-S test) indicated significant deviations
406 from perfect log-normality, likely due to large sample size and/or the presence of
407 outliers (see Appendices **Figure A1**). In contrast, pigments such as Zea, Perid and the
408 Fuco derivatives exhibited more variable distributions and greater heterogeneity among
409 samples. The histograms for the sea-ice samples (**Figure 6**, grey plots), had much more
410 variability in the distribution of concentrations. This is likely also related to smaller
411 sample size for sea-ice samples.



412

413 **Figure 6.** Frequency histograms displaying log-scaled pigment concentrations. Water samples are shown in blue and
414 sea-ice samples are shown in grey. x-axis represents actual pigment concentrations. Note the different ranges for y-
415 axis comparing water and sea-ice samples.

416

417 4. Data Availability

418 All datasets used in this paper have been compiled into a single repository, accessible
419 using DOI: <https://doi.org/10.11583/DTU.29445104> (Heidemann et al., 2026).

420

421 5. Conclusions

422 Photosynthetic and accessory pigments serve as indicators of community structure and
423 biomass, and are important oceanographic variables for understanding ocean ecology,
424 as they can also support assessment of biogeochemical cycling. Yet, datasets reporting
425 concentrations of those pigments remain sparse in the Arctic region. To address this
426 gap, we compiled, filtered, standardised and harmonised 10,798 pigment samples from
427 HPLC, including water (n = 10,095) and sea-ice samples (n = 703), collected during 77
428 research cruises spanning from 2000 to 2024 across 14 defined Arctic and sub-Arctic
429 regions. Sampling frequency varied by year, with peak efforts in 2002, 2009, 2016 and
430 2020. These years correspond to major multidisciplinary research projects and
431 international initiatives such as the International Polar Year (IPY). Seasonally, most
432 samples were collected during spring and summer months in the upper water column.

433 Within the available dataset, Chl-a was found in higher concentrations in sea-ice
434 samples compared to water samples, on average. However, for accessory pigments,
435 concentrations were generally found to be lower in sea-ice samples. Despite this, the



436 highest concentration of Chl-*a* across the dataset, 32.76 µg/L, was recorded for a water
 437 sample in the Chukchi Sea. Other areas that exhibited elevated Chl-*a* concentrations
 438 were spread across the Arctic marginal seas such as the Fram Strait, Barents Sea,
 439 Beaufort Sea and Labrador Sea. Interestingly, among the eight marker pigments, Fuco
 440 consistently had the highest pigment to Chl-*a* ratios, particularly during winter months,
 441 followed by a decline through summer and early autumn. For the sea-ice samples, the
 442 only accessory pigments with high ratios were Fuco and Chl-*b*.

443 Our comprehensive phytoplankton and sea-ice algal HPLC-based pigment dataset
 444 provides valuable insights into the research effort in the Arctic Ocean. Furthermore, it
 445 offers important observations on spatial and temporal patterns of primary producers
 446 supporting large-scale environmental research in the Arctic across over two decades of
 447 sampling efforts.

448

449 Appendices

450

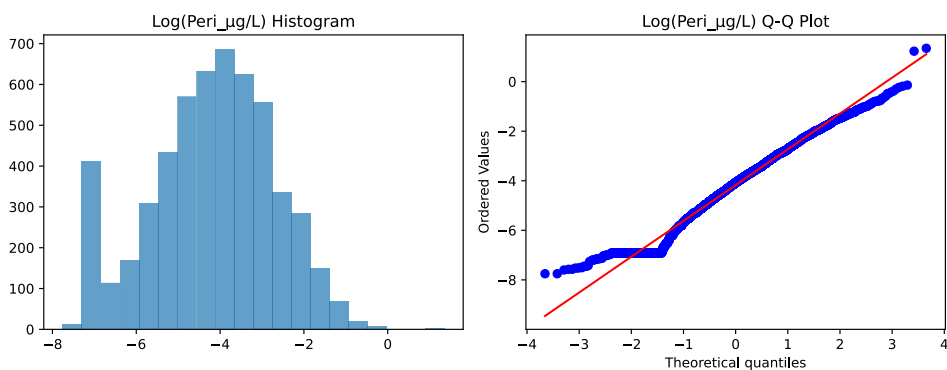
451 **Table A1.** *Pigment concentration statistics for all included measured pigments,*
 452 *separated by sample type and summarised across all cruises. For each pigment and*
 453 *environment, the table reports the 5th percentile, 95th percentile, mean, median and*
 454 *standard deviation (Std).*

Parameter / Pigment	Water Samples (µg/L)					Sea-ice Samples (µg/L)				
	5 th percentile	95 th percentile	Mean	Median	Std	5 th percentile	95 th percentile	Mean	Median	Std
Chl c3	0.000	0.232	0.054	0.014	0.116	0.000	0.051	0.014	0.000	0.053
Chl c1c2	0.000	0.652	0.146	0.048	0.295	0.000	0.365	0.101	0.035	0.254
Chl c1	0.000	0.031	0.009	0.000	0.061	0.000	0.000	0.000	0.000	0.007
Chlide a	0.000	0.062	0.015	0.000	0.078	0.000	0.007	0.002	0.000	0.022
Peri	0.000	0.105	0.021	0.001	0.072	0.000	0.057	0.016	0.000	0.078
Phide a	0.000	0.132	0.028	0.000	0.147	0.000	0.437	0.132	0.000	0.821
But-fuco	0.000	0.080	0.020	0.007	0.040	0.000	0.005	0.001	0.000	0.008
Fuco	0.003	1.493	0.357	0.106	0.853	0.000	1.392	0.367	0.063	1.120
Neo	0.000	0.022	0.005	0.000	0.010	0.000	0.014	0.002	0.000	0.010
Pras	0.000	0.053	0.011	0.000	0.025	0.000	0.005	0.001	0.000	0.006
Viola	0.000	0.027	0.007	0.002	0.012	0.000	0.034	0.010	0.000	0.049
Hex-fuco	0.000	0.434	0.092	0.019	0.180	0.000	0.011	0.002	0.000	0.010
Diadino	0.000	0.232	0.058	0.020	0.108	0.000	0.239	0.052	0.000	0.208
Allo	0.000	0.061	0.014	0.003	0.031	0.000	0.016	0.004	0.000	0.020
Diato	0.000	0.025	0.005	0.000	0.016	0.000	0.063	0.010	0.000	0.036
Zea	0.000	0.030	0.008	0.001	0.025	0.000	0.009	0.003	0.000	0.022
Lut	0.000	0.011	0.003	0.000	0.012	0.000	0.025	0.009	0.000	0.069
bacterio chl a	0.000	0.000	0.000	0.000	0.001	0.000	0.000	0.000	0.000	0.000
DV Chl b	0.000	0.000	0.000	0.000	0.004	0.000	0.000	0.000	0.000	0.000
Chl-b	0.000	0.207	0.059	0.033	0.091	0.000	0.158	0.037	0.000	0.109
DV Chl a	0.000	0.000	0.001	0.000	0.007	0.000	0.000	0.000	0.000	0.000
Chl-a	0.017	3.789	0.997	0.417	1.855	0.022	2.292	0.639	0.179	1.746
Phytin a	0.000	0.034	0.007	0.000	0.047	0.000	0.000	0.007	0.000	0.048
alphabetaCar	0.000	0.067	0.018	0.006	0.032	0.000	0.085	0.017	0.000	0.064

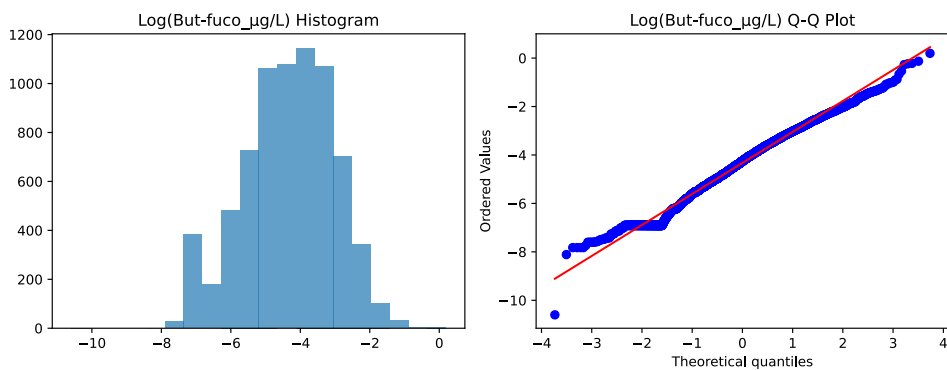
455



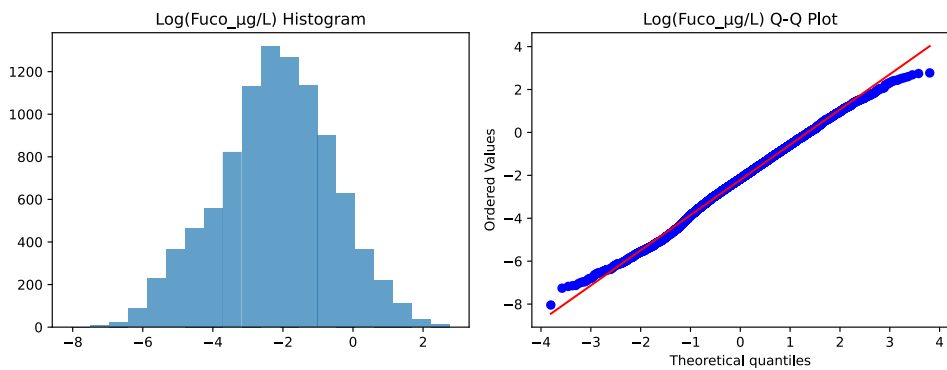
456 **Figure A1.** Histogram and Q-Q plots performed for each marker pigment on
457 standardised and log-transformed data. For each pigment, a histogram and a Q-Q plot
458 are visualized to assess normality. All Kolmogorov-Smirnov (K-S) p-values were below
459 0.05 test, indicating that the data deviates from a normal distribution.



460



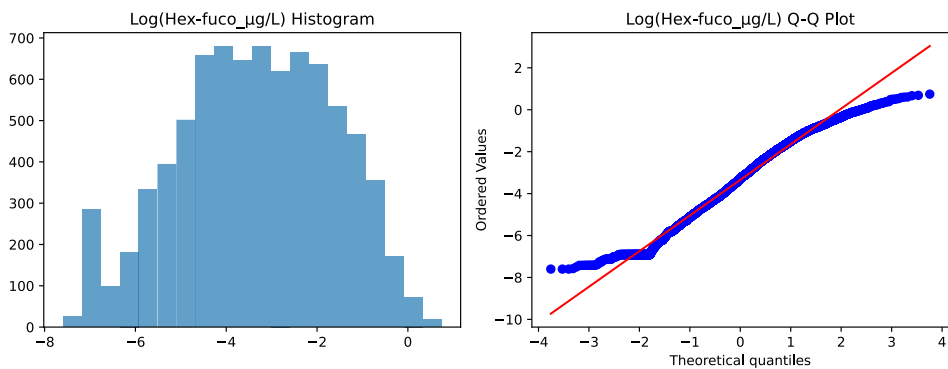
461



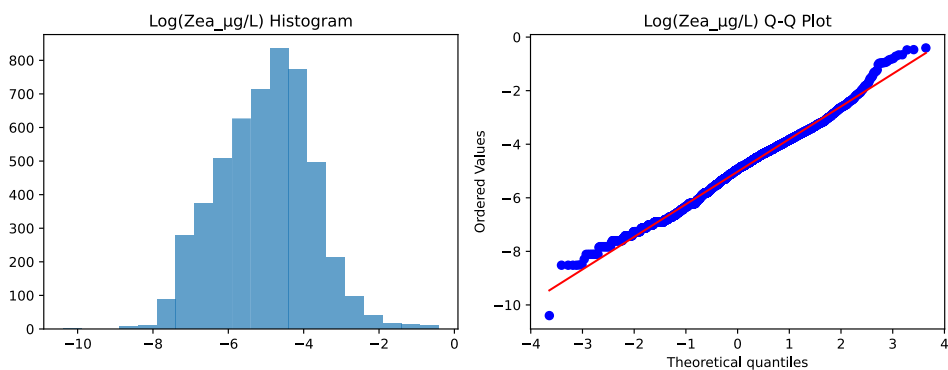
462

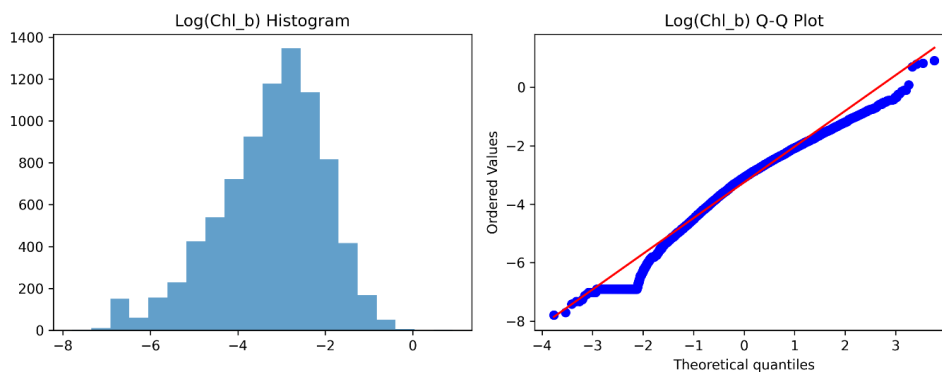


463

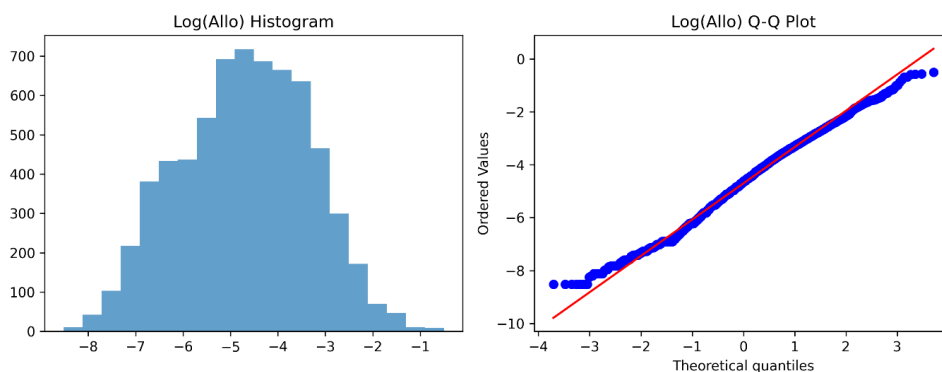


464





465



466

467

468 Author contributions

469 ACH consolidated the data, harmonized and standardised the dataset, performed the
470 data analysis, generated plots and developed the manuscript.

471 AH conceived the study idea, provided relevant expertise, contributed data, facilitated
472 key contacts and data sources and contributed to revising and improving the data
473 analysis and manuscript.

474 RG-A provided relevant expertise and contributed to conceiving the study idea, revising
475 and improving the data analysis and manuscript.

476 PA, AB (Astrid Bracher), GC, GD, KDD, AF, GMF, JH (Jacob Høyer), MI, AJ, TJP, PK, YL, AM
477 (Atsushi Matsuoka), AM (Alenya Merz), CJM, EO, IP, MP, JSE, AT, GV, HX and EJY
478 contributed data, provided relevant expertise and revised the manuscript.

479 AB (Atreya Basu) and JH (Jiwoon Hwang) provided relevant expertise and revised the
480 manuscript.

481



482 Acknowledgement

483 ACH and RG-A were supported by the Independent Research Fund Denmark, through
484 the project WaterColor (Gran No. 4251-00058B). RG-A was also supported by the
485 European Union’s Horizon Europe research and innovation program under Grant
486 Agreement No. 101136480 (SEA-Quester).

487 PA was supported by the Research Council of Norway (project no. 244646) and the
488 Ministry of Foreign Affairs, Norway, through the ID Arctic project.

489 AM was supported by NASA PACE (grant #: 80NSSC26K0091) and JAXA’s GCOM-C/SGLI
490 (25RT000334) projects.

491 YL was supported by Korea Institute of Marine Science and Technology Promotion
492 (KIMST) grant funded by the Ministry of Oceans and Fisheries (KIMST RS-2021-
493 KS211500, Korea-Arctic Ocean Warming and Response of Ecosystem, KOPRI).

494 KDD, JSE and PK were supported by a project funded by the Polish National Science
495 Centre (NCN) OPUS26 project OptiCal-Green (2023/51/B/ST10/01344) granted to PK.
496 Additional funding has been provided by the European Union’s Horizon Europe research
497 and innovation program under Grant Agreement No. 101136480 (SEA-Quester) and
498 under Grant Agreement No. 101136748 (BioEcoOcean), as well as the statutory
499 research program of the Institute of Oceanology, Polish Academy of Sciences (tasks I.2
500 and II.5). The ship time on board of r/v Kronprins Haakon was provided by the Norwegian
501 Polar Institute, Tromsø, Norway.

502 AB and HX were supported by the Helmholtz Infrastructure Initiative FRAM, German
503 Research Foundation (DFG) “Transregional Collaborative Research Center ArctiC
504 Amplification: Climate Relevant Atmospheric and SurfaCe Processes and Feedback
505 Mechanisms (AC)3” (Project C03), Copernicus Marine – Innovation Service Evolution
506 R&D Project ML-PhyTAO (23138L03D-COP-INNO SCI-9000), and the ESA project Phyto-
507 CCI(4000147645/25/I-LR). We thank the captain, the crew and all scientists of RV
508 Polarstern expeditions PS93-2, PS99-2, PS107, PS121, PS126, PS131, PS136 and
509 PS143-2 for their support in preparation and on board the expeditions.

510 IP was supported by the PoF III & IV program providing ship time on RV Polarstern
511 [Changing Earth –Sustaining our Future, Topic 6.1 of the Helmholtz Association]

512 AT was supported by the Helmholtz Young Investigator Group SiDe-Effect (VH-NG-1600)
513 awarded to Prof. Mar Fernández-Méndez. PS138 (ArcWatch I) was supported by the
514 Helmholtz Research Programme “Changing Earth – Sustaining our Future” Topic 6,
515 Subtopics 1, 2 and 3 (Grant No. AWI_PS138_02).

516

517



518 References

- 519 Ardyna, M. and Arrigo, K. R.: Phytoplankton dynamics in a changing Arctic Ocean, *Nat.*
520 *Clim. Change*, 10, 892–903, <https://doi.org/10.1038/s41558-020-0905-y>, 2020.
- 521 Arrigo, K. R. and van Dijken, G. L.: Continued increases in Arctic Ocean primary
522 production, *Synth. Arct. Res. SOAR*, 136, 60–70,
523 <https://doi.org/10.1016/j.pocean.2015.05.002>, 2015.
- 524 Artuso, F, Canuti, E, Cataldi, D, Costa Goela, P, Grung, M, Ras, J, and Röttgers, R:
525 HPLC/DAD intercomparison on phytoplankton pigments (HIP-1, HIP-2, HIP-3 and HIP-4),
526 Publications Office of the European Union, 2016.
- 527 Bidigare, R. R., Van Heukelem, L., and Trees, C. C.: HPLC phytoplankton pigments:
528 sampling, laboratory methods, and quality assurance procedures, *Ocean Opt. Protoc.*
529 *Satell. Ocean Color Sens. Valid. Revis.*, 3, 258–268, 2002.
- 530 Blais, M., Ardyna, M., Gosselin, M., Dumont, D., Bélanger, S., Tremblay, J.-É., Gratton, Y.,
531 Marchese, C., and Poulin, M.: Contrasting interannual changes in phytoplankton
532 productivity and community structure in the coastal Canadian Arctic Ocean, *Limnol.*
533 *Oceanogr.*, 62, 2480–2497, <https://doi.org/10.1002/lno.10581>, 2017.
- 534 Bonilla, S., Rautio, M., and Vincent, W. F.: Phytoplankton and phytobenthos pigment
535 strategies: implications for algal survival in the changing Arctic, *Polar Biol.*, 32, 1293–
536 1303, <https://doi.org/10.1007/s00300-009-0626-1>, 2009.
- 537 Bracher, A., Vountas, M., Dinter, T., Burrows, J. P., Röttgers, R., and Peeken, I.:
538 Quantitative observation of cyanobacteria and diatoms from space using PhytoDOAS
539 on SCIAMACHY data, *Biogeosciences*, 6, 751–764, [https://doi.org/10.5194/bg-6-751-](https://doi.org/10.5194/bg-6-751-2009)
540 2009, 2009.
- 541 Bracher, A., Bouman, H. A., Brewin, R. J. W., Bricaud, A., Brotas, V., Ciotti, A. M.,
542 Clementson, L., Devred, E., Di Cicco, A., Dutkiewicz, S., Hardman-Mountford, N. J.,
543 Hickman, A. E., Hieronymi, M., Hirata, T., Losa, S. N., Mouw, C. B., Organelli, E., Raitos,
544 D. E., Uitz, J., Vogt, M., and Wolanin, A.: Obtaining Phytoplankton Diversity from Ocean
545 Color: A Scientific Roadmap for Future Development, *Front. Mar. Sci.*, Volume 4-2017,
546 <https://doi.org/10.3389/fmars.2017.00055>, 2017.
- 547 Bracher, A., Soppa, M. A., Gege, P., Losa, S. N., Silva, B., Steinmetz, F., and Droscher, I.:
548 Extension of Atmospheric Correction Polymer to Hyperspectral Sensors: Application to
549 HICO and First Results for DESIS Data,
550 <https://doi.org/10.1109/IGARSS47720.2021.9553568>, 2021.
- 551 Brunet, C., Johnsen, G., Lavaud, J., and Roy, S.: Pigments and photoacclimation
552 processes, in: *Phytoplankton Pigments: Characterization, Chemotaxonomy and*
553 *Applications in Oceanography*, 2011.
- 554 Bruyant, F., Amiraux, R., Amyot, M.-P., Archambault, P., Artigue, L., Barbedo de Freitas,
555 L., Bécu, G., Bélanger, S., Bourgain, P., Bricaud, A., Brouard, E., Brunet, C., Burgers, T.,



- 556 Caleb, D., Chalut, K., Claustre, H., Cornet-Barthaux, V., Coupel, P., Cusa, M., Cusset, F.,
557 Dadaglio, L., Davelaar, M., Deslongchamps, G., Dimier, C., Dinasquet, J., Dumont, D.,
558 Else, B., Eulaers, I., Ferland, J., Filteau, G., Forget, M.-H., Fort, J., Fortier, L., Galí, M.,
559 Gallinari, M., Garbus, S.-E., Garcia, N., Gérikas Ribeiro, C., Gombault, C., Gourvil, P.,
560 Goyens, C., Grant, C., Grondin, P.-L., Guillot, P., Hillion, S., Hussherr, R., Joux, F., Joy-
561 Warren, H., Joyal, G., Kieber, D., Lafond, A., Lagunas, J., Lajeunesse, P., Lalande, C.,
562 Larivière, J., Le Gall, F., Leblanc, K., Leblanc, M., Legras, J., Lévesque, K., Lewis, K.-M.,
563 Leymarie, E., Leynaert, A., Linkowski, T., Lizotte, M., Lopes dos Santos, A., Marec, C.,
564 Marie, D., Massé, G., Massicotte, P., Matsuoka, A., Miller, L. A., Mirshak, S., Morata, N.,
565 Moriceau, B., Morin, P.-I., Morisset, S., Mosbech, A., Mucci, A., Nadaï, G., Nozais, C.,
566 Obernosterer, I., Paire, T., Panagiotopoulos, C., Parenteau, M., Pelletier, N., Picheral, M.,
567 Quéguiner, B., Raimbault, P., Ras, J., Rehm, E., Ribot Lacosta, L., Rontani, J.-F., Saint-
568 Béat, B., Sansoulet, J., Sardet, N., Schmechtig, C., Sciandra, A., Sempéré, R., et al.: The
569 Green Edge cruise: investigating the marginal ice zone processes during late spring and
570 early summer to understand the fate of the Arctic phytoplankton bloom, *Earth Syst. Sci.*
571 *Data*, 14, 4607–4642, <https://doi.org/10.5194/essd-14-4607-2022>, 2022.
- 572 Campbell, R. G., Sherr, E. B., Ashjian, C. J., Plourde, S., Sherr, B. F., Hill, V., and
573 Stockwell, D. A.: Mesozooplankton prey preference and grazing impact in the western
574 Arctic Ocean, *Deep Sea Res. Part II Top. Stud. Oceanogr.*, 56, 1274–1289,
575 <https://doi.org/10.1016/j.dsr2.2008.10.027>, 2009.
- 576 Canuti, E.: Phytoplankton pigment in situ measurements uncertainty evaluation: an
577 HPLC interlaboratory comparison with a European-scale dataset, *Front. Mar. Sci.*, 10,
578 <https://doi.org/10.3389/fmars.2023.1197311>, 2023.
- 579 Canuti, E., Grung, J., Röttgers, M., Goela, C., and Artuso, P.: HPLC/DAD Intercomparison
580 on Phytoplankton Pigments (HIP-1, HIP-2, HIP-3 and HIP-4),
581 <https://doi.org/10.2788/47099>, 2016.
- 582 Cetinić, I., Rousseaux, C. S., Carroll, I. T., Chase, A. P., Kramer, S. J., Werdell, P. J., Siegel,
583 D. A., Dierssen, H. M., Catlett, D., Neeley, A., Soto Ramos, I. M., Wolny, J. L., Sadoff, N.,
584 Urquhart, E., Westberry, T. K., Stramski, D., Pahlevan, N., Seegers, B. N., Sirk, E., Lange,
585 P. K., Vandermeulen, R. A., Graff, J. R., Allen, J. G., Gaube, P., McKinna, L. I. W.,
586 McKibben, S. M., Binding, C. E., Calzado, V. S., and Sayers, M.: Phytoplankton
587 composition from sPACE: Requirements, opportunities, and challenges, *Remote Sens.*
588 *Environ.*, 302, 113964, <https://doi.org/10.1016/j.rse.2023.113964>, 2024.
- 589 Chamberlain, E. J., Balmonte, J. P., Torstensson, A., Fong, A. A., Snoeijs-Leijonmalm, P.,
590 and Bowman, J. S.: Impacts of sea ice melting procedures on measurements of
591 microbial community structure, *Elem. Sci. Anthr.*, 10, 00017,
592 <https://doi.org/10.1525/elementa.2022.00017>, 2022.
- 593 Claustre, H., Hooker, S. B., Van Heukelem, L., Berthon, J.-F., Barlow, R., Ras, J.,
594 Sessions, H., Targa, C., Thomas, C. S., van der Linde, D., and Marty, J.-C.: An
595 intercomparison of HPLC phytoplankton pigment methods using in situ samples:
596 application to remote sensing and database activities, *Mar. Chem.*, 85, 41–61,
597 <https://doi.org/10.1016/j.marchem.2003.09.002>, 2004.



- 598 Coupel, P., Jin, H. Y., Joo, M., Horner, R., Bouvet, H. A., Sicre, M.-A., Gascard, J.-C.,
599 Chen, J. F., Garçon, V., and Ruiz-Pino, D.: Phytoplankton distribution in unusually low
600 sea ice cover over the Pacific Arctic, *Biogeosciences*, 9, 4835–4850,
601 <https://doi.org/10.5194/bg-9-4835-2012>, 2012.
- 602 Coupel, P., Matsuoka, A., Ruiz-Pino, D., Gosselin, M., Marie, D., Tremblay, J.-É., and
603 Babin, M.: Pigment signatures of phytoplankton communities in the Beaufort Sea,
604 *Biogeosciences*, 12, 991–1006, <https://doi.org/10.5194/bg-12-991-2015>, 2015.
- 605 El Hourany, R., Abboud-Abi Saab, M., Faour, G., Aumont, O., Crépon, M., and Thiria, S.:
606 Estimation of Secondary Phytoplankton Pigments From Satellite Observations Using
607 Self-Organizing Maps (SOMs), *J. Geophys. Res. Oceans*, 124, 1357–1378,
608 <https://doi.org/10.1029/2018JC014450>, 2019.
- 609 El Hourany, R., Pierella Karlusich, J., Zinger, L., Loisel, H., Levy, M., and Bowler, C.:
610 Linking satellites to genes with machine learning to estimate phytoplankton community
611 structure from space, *Ocean Sci.*, 20, 217–239, [https://doi.org/10.5194/os-20-217-](https://doi.org/10.5194/os-20-217-2024)
612 [2024](https://doi.org/10.5194/os-20-217-2024), 2024.
- 613 England, M. R., Eisenman, I., Lutsko, N. J., and Wagner, T. J. W.: The Recent Emergence
614 of Arctic Amplification, *Geophys. Res. Lett.*, 48, e2021GL094086,
615 <https://doi.org/10.1029/2021GL094086>, 2021.
- 616 Falkowski, P. G.: The role of phytoplankton photosynthesis in global biogeochemical
617 cycles, *Photosynth. Res.*, 39, 235–258, <https://doi.org/10.1007/BF00014586>, 1994.
- 618 Flores, H., Veyssi re, G., Castellani, G., Wilkinson, J., Hoppmann, M., Karcher, M.,
619 Valcic, L., Cornils, A., Geoffroy, M., Nicolaus, M., Niehoff, B., Priou, P., Schmidt, K., and
620 Stroeve, J.: Sea-ice decline could keep zooplankton deeper for longer, *Nat. Clim.*
621 *Change*, 13, 1122–1130, <https://doi.org/10.1038/s41558-023-01779-1>, 2023.
- 622 Fragoso, G. M., Poulton, A. J., Yashayaev, I. M., Head, E. J. H., and Purdie, D. A.: Spring
623 phytoplankton communities of the Labrador Sea (2005–2014): pigment signatures,
624 photophysiology and elemental ratios, *Biogeosciences*, 14, 1235–1259,
625 <https://doi.org/10.5194/bg-14-1235-2017>, 2017.
- 626 Freer, J. J., Daase, M., and Tarling, G. A.: Modelling the biogeographic boundary shift of
627 *Calanus finmarchicus* reveals drivers of Arctic Atlantification by subarctic zooplankton,
628 *Glob. Change Biol.*, 28, 429–440, <https://doi.org/10.1111/gcb.15937>, 2022.
- 629 Gege, P.: The water color simulator WASI: an integrating software tool for analysis and
630 simulation of optical in situ spectra, *Comput. Geosci.*, 30, 523–532,
631 <https://doi.org/10.1016/j.cageo.2004.03.005>, 2004.
- 632 Gege, P.: WASI-2D: A software tool for regionally optimized analysis of imaging
633 spectrometer data from deep and shallow waters, *Comput. Geosci.*, 62, 208–215,
634 <https://doi.org/10.1016/j.cageo.2013.07.022>, 2014.



- 635 Gosselin, M., Rysgaard, S., Lavaud, J., Else, B., Galindo, V., Mundy, C. J., Ehn, J., and
636 Babin, M.: Pigment composition and photoprotection of Arctic sea ice algae during
637 spring, *Mar. Ecol. Prog. Ser.*, 585, 49–69, 2017.
- 638 Gradinger, R.: Sea-ice algae: Major contributors to primary production and algal
639 biomass in the Chukchi and Beaufort Seas during May/June 2002, *Deep Sea Res. Part II*
640 *Top. Stud. Oceanogr.*, 56, 1201–1212, <https://doi.org/10.1016/j.dsr2.2008.10.016>, 2009.
- 641 Hayward, A., Pinkerton, M. H., and Gutierrez-Rodriguez, A.: phytoclass: A pigment-
642 based chemotaxonomic method to determine the biomass of phytoplankton classes,
643 *Limnol. Oceanogr. Methods*, 21, 220–241, <https://doi.org/10.1002/lom3.10541>, 2023.
- 644 Hayward, A., Pinkerton, M. H., Wright, S. W., Gutiérrez-Rodriguez, A., and Law, C. S.:
645 Twenty-six years of phytoplankton pigments reveal a circumpolar Class Divide around
646 the Southern Ocean, *Commun. Earth Environ.*, 5, 92, [https://doi.org/10.1038/s43247-](https://doi.org/10.1038/s43247-024-01261-6)
647 024-01261-6, 2024.
- 648 Hayward, A., Wright, S. W., Carroll, D., Law, C. S., Wongpan, P., Gutiérrez-Rodriguez, A.,
649 and Pinkerton, M. H.: Antarctic phytoplankton communities restructure under shifting
650 sea-ice regimes, *Nat. Clim. Change*, <https://doi.org/10.1038/s41558-025-02379-x>,
651 2025.
- 652 Heidemann, A. C., Hayward, A., Assmy, P., Basu, A., Bracher, A., Castellani, G., Ditullio,
653 G., Dragańska-Deja, K., Fujiwara, A., Fragoso, G. M., Høyer, J., Hwang, J., Iversen, M.,
654 von Jackowski, A., Juul-Pedersen, T., Kowalczyk, P., Lee, Y., Matsuoka, A., Merz, A.,
655 Mundy, C. J., Ostermann, E., Pinkerton, M. H., Peeken, I., Stoń-Egiert, J., Thielecke, A. U.,
656 Veysiere, G., Xi, H., Yang, E. J., and Gonçalves-Araujo, R.: Consolidated Arctic Pigments
657 (2000 to 2024), <https://doi.org/10.11583/DTU.29445104>, 2026.
- 658 Hooker, S. B., Heukelem, L., Thomas, C. S., Claustre, H., Ras, J., Barlow, R., Sessions,
659 H., Schlüter, L., Perl, J., Trees, C., Stuart, V., Head, E., Clementson, L., Fishwick, J.,
660 Llewellyn, C., and Aiken, J.: The Second SeaWiFS HPLC Analysis Round-robin
661 Experiment (SeaHARRE-2), National Aeronautics and Space Administration, Goddard
662 Space Flight Center, 124 pp., 2005.
- 663 Hooker, S. B., Clementson, L., Thomas, C. S., Schlüter, L., Allerup, M., Ras, J., Claire, N.,
664 Cullen, J., Kienast, M., Kozłowski, W., Vernet, M., Chakraborty, S., Lohrenz, S., Tuel, M.,
665 Redalje, D., Cartaxana, P., Mendes, C. R., Brotas, V., Matondkar, S. G. P., Parab, S. G.,
666 Neeley, A., and Egeland, E. S.: The Fifth SeaWiFS HPLC Analysis Round-Robin
667 Experiment (SeaHARRE-5), 2012.
- 668 Hu, C.: Hyperspectral reflectance spectra of floating matters derived from
669 Hyperspectral Imager for the Coastal Ocean (HICO) observations, *Earth Syst. Sci. Data*,
670 14, 1183–1192, <https://doi.org/10.5194/essd-14-1183-2022>, 2022.
- 671 Hwang, J.: Preliminarily annotated phytoplankton lipids from Polar Cod Connectivity
672 Cruise 2022, <https://doi.org/10.5281/zenodo.15085544>, 2025.



- 673 Jeffrey, S. W., Wright, S. W., and Zapata, M.: Recent advances in HPLC pigment analysis
674 of phytoplankton, *Mar. Freshw. Res.*, 50, 879–896, 1999.
- 675 Kramer, S. J., Siegel, D. A., Maritorena, S., and Catlett, D.: Modeling surface ocean
676 phytoplankton pigments from hyperspectral remote sensing reflectance on global
677 scales, *Remote Sens. Environ.*, 270, 112879, <https://doi.org/10.1016/j.rse.2021.112879>,
678 2022.
- 679 Losa, S. N., Soppa, M. A., Dinter, T., Wolanin, A., Brewin, R. J. W., Bricaud, A., Oelker, J.,
680 Peeken, I., Gentili, B., Rozanov, V., and Bracher, A.: Synergistic Exploitation of Hyper-
681 and Multi-Spectral Precursor Sentinel Measurements to Determine Phytoplankton
682 Functional Types (SynSenPFT), *Front. Mar. Sci.*, 4,
683 <https://doi.org/10.3389/fmars.2017.00203>, 2017.
- 684 Massicotte, P., Amiraux, R., Amyot, M.-P., Archambault, P., Ardyna, M., Arnaud, L.,
685 Artigue, L., Aubry, C., Ayotte, P., Bécu, G., Bélanger, S., Benner, R., Bittig, H. C., Bricaud,
686 A., Brossier, É., Bruyant, F., Chauvaud, L., Christiansen-Stowe, D., Claustre, H., Cornet-
687 Barthaux, V., Coupel, P., Cox, C., Delaforge, A., Dezutter, T., Dimier, C., Domine, F.,
688 Dufour, F., Dufresne, C., Dumont, D., Ehn, J., Else, B., Ferland, J., Forget, M.-H., Fortier,
689 L., Galí, M., Galindo, V., Gallinari, M., Garcia, N., Gérikas Ribeiro, C., Gourdal, M.,
690 Gourvil, P., Goyens, C., Grondin, P.-L., Guillot, P., Guilmette, C., Houssais, M.-N., Joux,
691 F., Lacour, L., Lacour, T., Lafond, A., Lagunas, J., Lalande, C., Laliberté, J., Lambert-
692 Girard, S., Larivière, J., Lavaud, J., LeBaron, A., Leblanc, K., Le Gall, F., Legras, J., Lemire,
693 M., Levasseur, M., Leymarie, E., Leynaert, A., Lopes dos Santos, A., Lourenço, A., Mah,
694 D., Marec, C., Marie, D., Martin, N., Marty, C., Marty, S., Massé, G., Matsuoka, A.,
695 Matthes, L., Moriceau, B., Muller, P.-E., Mundy, C.-J., Neukermans, G., Oziel, L.,
696 Panagiotopoulos, C., Pangrazi, J.-J., Picard, G., Picheral, M., Pinczon du Sel, F.,
697 Pogorzelec, N., Probert, I., Quéguiner, B., Raimbault, P., Ras, J., Rehm, E., Reimer, E.,
698 Rontani, J.-F., Rysgaard, S., Saint-Béat, B., Sampei, M., Sansoulet, J., Schmechtig, C.,
699 Schmidt, S., et al.: Green Edge ice camp campaigns: understanding the processes
700 controlling the under-ice Arctic phytoplankton spring bloom, *Earth Syst. Sci. Data*, 12,
701 151–176, <https://doi.org/10.5194/essd-12-151-2020>, 2020.
- 702 Mattei, F. and Scardi, M.: Collection and analysis of a global marine phytoplankton
703 primary-production dataset, *Earth Syst. Sci. Data*, 13, 4967–4985,
704 <https://doi.org/10.5194/essd-13-4967-2021>, 2021.
- 705 Mendes, C. R., Cartaxana, P., and Brotas, V.: HPLC determination of phytoplankton and
706 microphytobenthos pigments: comparing resolution and sensitivity of a C18 and a C8
707 method, *Limnol. Oceanogr. Methods*, 5, 363–370,
708 <https://doi.org/10.4319/lom.2007.5.363>, 2007.
- 709 Miller, L. A., Fripiat, F., Else, B. G. T., Bowman, J. S., Brown, K. A., Collins, R. E., Ewert, M.,
710 Fransson, A., Gosselin, M., Lannuzel, D., Meiners, K. M., Michel, C., Nishioka, J.,
711 Nomura, D., Papadimitriou, S., Russell, L. M., Sørensen, L. L., Thomas, D. N., Tison, J.-
712 L., van Leeuwe, M. A., Vancoppenolle, M., Wolff, E. W., and Zhou, J.: Methods for
713 biogeochemical studies of sea ice: The state of the art, caveats, and recommendations,
714 *Elem. Sci. Anthr.*, 3, 000038, <https://doi.org/10.12952/journal.elementa.000038>, 2015.



- 715 Miller, P.: Multi-spectral front maps for automatic detection of ocean colour features
716 from SeaWiFS, *Int. J. Remote Sens.*, 25, 1437–1442,
717 <https://doi.org/10.1080/01431160310001592409>, 2004.
- 718 Negrete-García, G., Luo, J. Y., Petrik, C. M., Manizza, M., and Barton, A. D.: Changes in
719 Arctic Ocean plankton community structure and trophic dynamics on seasonal to
720 interannual timescales, *Biogeosciences*, 21, 4951–4973, <https://doi.org/10.5194/bg-21-4951-2024>, 2024.
- 722 Nieke, J., Mavrocordatos, C., Donlon, C., Berruti, B., Garnier, T., Riti, J.-B., and Delclaud,
723 Y.: Ocean and Land Color Imager on Sentinel-3, in: *Optical Payloads for Space Missions*,
724 John Wiley & Sons, Ltd, 223–245, <https://doi.org/10.1002/9781118945179.ch10>, 2015.
- 725 Nieke, J., Despoisse, L., Gabriele, A., Weber, H., Strese, H., Ghasemi, N., Gascon, F.,
726 Alonso, K., Boccia, V., Tsonevska, B., Choukroun, P., Ottavianelli, G., and Celesti, M.:
727 The copernicus hyperspectral imaging mission for the environment (CHIME): an
728 overview of its mission, system and planning status, in: *Sensors, Systems, and Next-
729 Generation Satellites XXVII*, *Sensors, Systems, and Next-Generation Satellites XXVII*,
730 21–40, <https://doi.org/10.1117/12.2679977>, 2023.
- 731 Peloquin, J., Swan, C., Gruber, N., Vogt, M., Claustre, H., Ras, J., Uitz, J., Barlow, R.,
732 Behrenfeld, M., Bidigare, R., Dierssen, H., Ditullio, G., Fernandez, E., Gallienne, C., Gibb,
733 S., Goericke, R., Harding, L., Head, E., Holligan, P., Hooker, S., Karl, D., Landry, M.,
734 Letelier, R., Llewellyn, C. A., Lomas, M., Lucas, M., Mannino, A., Marty, J.-C., Mitchell, B.
735 G., Muller-Karger, F., Nelson, N., O'Brien, C., Prezelin, B., Repeta, D., Jr. Smith, W. O.,
736 Smythe-Wright, D., Stumpf, R., Subramaniam, A., Suzuki, K., Trees, C., Vernet, M.,
737 Wasmund, N., and Wright, S.: The MAREDAT global database of high performance liquid
738 chromatography marine pigment measurements, *Earth Syst. Sci. Data*, 5, 109–123,
739 <https://doi.org/10.5194/essd-5-109-2013>, 2013.
- 740 Pereira, L. and Gonçalves, A. M. M.: *Plankton Communities, BoD – Books on Demand*,
741 200 pp., 2022.
- 742 Quinlan, R., Douglas, M. S. V., and Smol, J. P.: Food web changes in arctic ecosystems
743 related to climate warming, *Glob. Change Biol.*, 11, 1381–1386,
744 <https://doi.org/10.1111/j.1365-2486.2005.00981.x>, 2005.
- 745 Roy, S., Llewellyn, C. A., Egeland, E. S., and Johnsen, G.: *Phytoplankton Pigments:
746 Characterization, Chemotaxonomy and Applications in Oceanography*, Cambridge
747 University Press, 891 pp., 2011.
- 748 Sadeghi, A., Dinter, T., Vountas, M., Taylor, B. B., Altenburg-Soppa, M., Peeken, I., and
749 Bracher, A.: Improvement to the PhytoDOAS method for identification of
750 coccolithophores using hyper-spectral satellite data, *Ocean Sci.*, 8, 1055–1070,
751 <https://doi.org/10.5194/os-8-1055-2012>, 2012.
- 752 Serra-Pompei, C., Ward, B. A., Pinti, J., Visser, A. W., Kiørboe, T., and Andersen, K. H.:
753 Linking Plankton Size Spectra and Community Composition to Carbon Export and Its



- 754 Efficiency, *Glob. Biogeochem. Cycles*, 36, e2021GB007275,
755 <https://doi.org/10.1029/2021GB007275>, 2022.
- 756 Simmons, L. J., Sandgren, C. D., and Berges, J. A.: Problems and pitfalls in using HPLC
757 pigment analysis to distinguish Lake Michigan phytoplankton taxa, *J. Gt. Lakes Res.*, 42,
758 397–404, <https://doi.org/10.1016/j.jglr.2015.12.006>, 2016.
- 759 Six, C., Ratin, M., Marie, D., and Corre, E.: Marine *Synechococcus* picocyanobacteria:
760 Light utilization across latitudes, *Proc. Natl. Acad. Sci.*, 118, e2111300118,
761 <https://doi.org/10.1073/pnas.2111300118>, 2021.
- 762 Stroeve, J. and Notz, D.: Changing state of Arctic sea ice across all seasons,
763 <https://doi.org/10.1088/1748-9326/aade56>, 2018.
- 764 Swan, C. M., Vogt, M., Gruber, N., and Laufkoetter, C.: A global seasonal surface ocean
765 climatology of phytoplankton types based on CHEMTAX analysis of HPLC pigments,
766 *Deep Sea Res. Part Oceanogr. Res. Pap.*, 109, 137–156,
767 <https://doi.org/10.1016/j.dsr.2015.12.002>, 2016.
- 768 Vidussi, F., Claustre, H., Manca, B. B., Luchetta, A., and Marty, J.-C.: Phytoplankton
769 pigment distribution in relation to upper thermocline circulation in the eastern
770 Mediterranean Sea during winter, *J. Geophys. Res. Oceans*, 106, 19939–19956,
771 <https://doi.org/10.1029/1999JC000308>, 2001.
- 772 Vonnahme, T. R., Chitkara, C., Krawczyk, D., Meire, L., Skogseth, R., Vader, A., and Juul-
773 Pedersen, T.: Abrupt decline of microplankton species richness linked to coastal inflow
774 in an Arctic fjord, *Limnol. Oceanogr.*, 70, 2688–2702, <https://doi.org/10.1002/lno.70159>,
775 2025.
- 776 Werdell, P. J., Franz, B., Poulin, C., Allen, J., Cairns, B., Caplan, S., Cetinić, I., Craig, S.,
777 Gao, M., Hasekamp, O., Ibrahim, A., Knobelspiesse, K., Mannino, A., Martins, J. V.,
778 McKinna, L., Meister, G., Patt, F., Proctor, C., Rajapakshe, C., Ramos, I. S., Rietjens, J.,
779 Sayer, A., and Sirk, E.: Life after launch: a snapshot of the first six months of NASA's
780 Plankton, Aerosol, Cloud, Ocean Ecosystem (PACE) mission, in: *Sensors, Systems, and*
781 *Next-Generation Satellites XXVIII, Sensors, Systems, and Next-Generation Satellites*
782 *XXVIII*, 70–84, <https://doi.org/10.1117/12.3033830>, 2024.
- 783 Wright, S. W. and Jeffrey, S. W.: Pigment Markers for Phytoplankton Production, in:
784 *Marine Organic Matter: Biomarkers, Isotopes and DNA*, edited by: Volkman, J. K.,
785 Springer Berlin Heidelberg, Berlin, Heidelberg, 71–104,
786 https://doi.org/10.1007/698_2_003, 2006.
- 787 Xi, H., Losa, S. N., Mangin, A., Soppa, M. A., Garnesson, P., Demaria, J., Liu, Y., d'Andon,
788 O. H. F., and Bracher, A.: Global retrieval of phytoplankton functional types based on
789 empirical orthogonal functions using CMEMS GlobColour merged products and further
790 extension to OLCI data, *Remote Sens. Environ.*, 240, 111704,
791 <https://doi.org/10.1016/j.rse.2020.111704>, 2020.



792 Xi, H., Peeken, I., Gomes, M., Brotas, V., Tilstone, G. H., Brewin, R. J. W., Dall’Olmo, G.,
793 Tracana, A., Alvarado, L. M. A., Murawski, S., Wiegmann, S., and Bracher, A.:
794 Phytoplankton pigment concentrations and phytoplankton groups measured on water
795 samples collected from various expeditions in the Atlantic Ocean from 71°S to 84°N,
796 <https://doi.org/10.1594/PANGAEA.954738>, 2023.

797 Zapata, M., Rodríguez, F., and Garrido, J. L.: Separation of chlorophylls and carotenoids
798 from marine phytoplankton: a new HPLC method using a reversed phase C8 column
799 and pyridine-containing mobile phases, *Mar. Ecol. Prog. Ser.*, 195, 29–45,
800 <https://doi.org/10.3354/meps195029>, 2000.

801

802

803